THE JOURNAL OF PHYSICAL CHEMISTRY B

pubs.acs.org/JPCB Article

Disulfide Chromophores Arise from Stereoelectronic Effects

Henry R. Kilgore and Ronald T. Raines*

Cite This: J. Phys. Chem. B 2020, 124, 3931−3935 Read Online

ACCESS | Metrics & More | Article Recommendations | Supporting Information

ABSTRACT: Bonds between sulfur atoms are prevalent in natural products, peptides, and proteins. Disulfide bonds have a distinct chromophore. The wavelength of their maximal absorbance varies widely, from 250 to 500 nm. Here, we demonstrate that this wavelength derives from stereoelectronic effects and is predictable using quantum chemistry. We also provide a sinusoidal equation, analogous to the Karplus equation, that relates the absorbance maximum and the C−S−S−C dihedral angle. These insights provide a facile means to characterize important attributes of disulfide bonds and to design disulfides with specified photophysical properties.

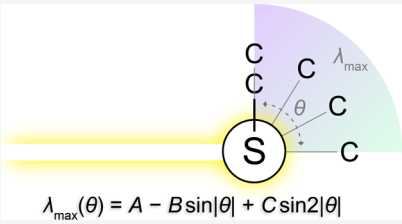

INTRODUCTION

Disulfide bonds between cysteine residues of proteins are pivotal in a variety of fundamental biological processes, including oxidative protein folding, redox homeostasis, and signal transduction.[1−6] Disulfide bonds are also key components of peptides[7−9] and natural products.[10−12] Noncovalent interactions, molecular conformation, and the local chemical environment are all known to influence the physicochemical properties of disulfide bonds.[13−18] We reasoned that these properties could also correlate with the interaction of disulfide bonds with light.

Early investigations into the disulfide chromophore resulted in a description of the mechanism of disulfide photolysis. In the 1950s, Calvin and his co-workers measured a quantum yield of up to $\Phi = 0.865$ for photolysis upon irradiation at the excitation maximum.[19,20] They proposed a mechanism involving photo-induced sulfur−sulfur bond scission to form two thiyl radicals. They found that the C−S−S−C dihedral angle and α-substituents modulate the frequency required to cleave the disulfide bond. The pattern that emerged from these early studies was simple—a more eclipsed conformation increases the energy (E) and decreases the wavelength ($\lambda \propto E^{-1}$) required to excite an electron from the ground state, $\mathbf{S_0}$, to the first excited state, $\mathbf{S_1}$. Notably, Calvin's work on the disulfide bond in lipoic acid led ultimately to his renowned investigations of photosynthesis.[21,22]

Extended Hückel theory has implicated electron−electron repulsion in hydrogen disulfide and dimethyl disulfide as the origin of the wavelength dependence of their chromophores.[23] This granular treatment matched early experimental data. For example, smaller R−S−S−R dihedral angles were found to correlate with higher energy sulfur−sulfur bond vibrations in Raman spectra.[14] Modern experimental investigations have described the excitation pathway more thoroughly.[24,25]

Here, we investigate the quantum origins of disulfide chromophores and ensuing consequences. We find that the excitation energy and thus the wavelength of maximal absorbance (λ_{max}) of a disulfide bond rely on stereoelectronic effects. Moreover, we demonstrate a correlation between the value of the C−S−S−C dihedral angle and that of λ_{max}. This correlation has important implications in the exploration and exploitation of disulfide bonds in chemical and biochemical systems.

MATERIALS AND METHODS

UV−Vis Spectroscopy. Lipoic acid and oxidized dithiothreitol (Cleland's reagent[26]) were obtained from Sigma−Aldrich (St. Louis, MO). UV−vis spectra of 10 mM oxidized lipoic acid and oxidized dithiothreitol were recorded in 20 mM BIS-TRIS buffer, pH 7.5, with an Agilent Cary 60 UV−vis spectrophotometer (Figure S1). Other experimental absorbance maxima are listed in Table S1.

Effect of the Dielectric Constant on UV−Vis Absorbance. Solutions of lipoic acid disulfide and dithiothreitol disulfide were prepared at 1 mM in water or dioxane. The absorbance of these solutions was measured before and after mixing in 1:3, 2:1, and 3:1 ratios. The dielectric constant of the five solutions was interpolated from literature data.[27]

Computational Methods. Quantum mechanical calculations were performed with Gaussian 16, revision C.01 from Gaussian (Wallington, CT) at the M06-2X/6-311+g(d,p) level of theory.[28] Ground-state ($\mathbf{S_0}$) geometries were found to possess no imaginary frequencies. Excited-state calculations were performed using time-dependent density functional theory (TD-DFT) as implemented in Gaussian 16, revision C.01. A total of 20 singlet-state excitations were calculated at the M06-2X/6-311+g(d,p) level of theory, and the lowest

Received: March 14, 2020
Revised: April 15, 2020
Published: April 15, 2020

ACS Publications © 2020 American Chemical Society

https://dx.doi.org/10.1021/acs.jpcb.0c02272
J. Phys. Chem. B 2020, 124, 3931−3935

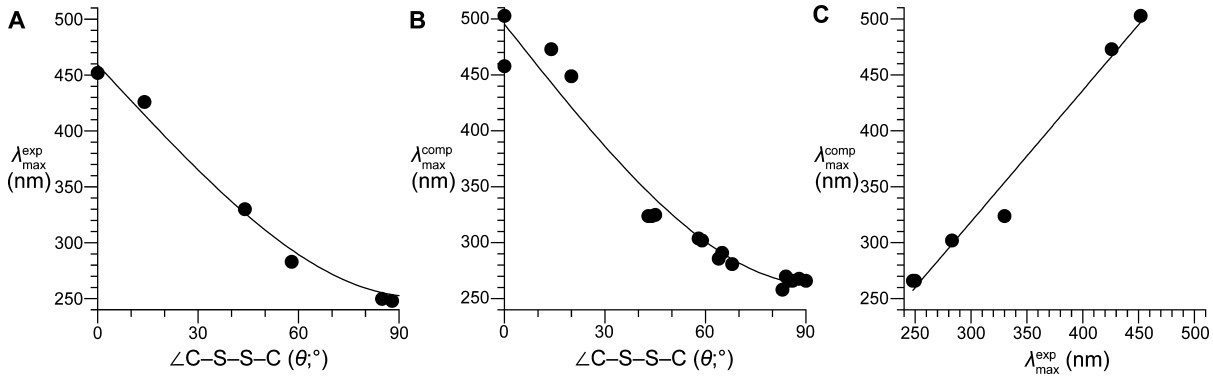

Figure 1. Relationships between experimental absorbance maxima, computed absorbance maxima, and computed C−S−S−C dihedral angles for cyclic disulfides containing 1−6 methylene groups. (A) Graph of the experimental absorbance maxima versus the computed C−S−S−C dihedral angle (M06-2X/6-311+G(d,p) level of theory). Data were fitted to eq 1 with A = 460 nm, B = 207 nm, and C = 8.42 nm; R^2 = 0.98. (B) Graph of the computed absorbance maxima versus the C−S−S−C dihedral angle. Data were fitted to eq 1 with A = 496 nm, B = 238 nm, and C = 8.98 nm; R^2 = 0.96. (C) Graph of the experimental absorbance maxima versus the computational absorbance maxima. R^2 = 0.98; slope = 1.17. Data are listed in Table S1.

energy excitation is reported as λ_{max}^{comp}. Visualization of the $S_0 \rightarrow S_1$ transition was achieved by employing Martin's natural transition orbitals as implemented in Gaussian 16, revision C.01.[29] Natural transition orbitals were visualized with GaussView 6 from Semichem (Shawnee Mission, KS),[30] using an iso-value of 0.045. Conformationally constrained calculations with diethyl disulfide were performed by optimizing the molecule while holding the C−S−S−C dihedral angle, θ, at a constant value. From these conformationally constrained calculations, values of $E - E_0$ were obtained by subtracting the energy of diethyl disulfide in the fully unconstrained conformation (E_0) from the conformationally constrained energy, E. Values of $\Delta G_{anomeric} = G_{anomeric} - G_{agnostic}$ were calculated from the difference in the free energies of symmetric anomeric and non-anomeric substituted dimethyl disulfides.

Data Analysis. Graphs of λ_{max}^{exp} versus θ (Figure 1A) and λ_{max}^{comp} versus θ (Figure 1B) were fitted to a sinusoidal function with MATLAB R2018A software from MathWorks (Natick, MA).

■ RESULTS AND DISCUSSION

To begin, we considered cyclic disulfides. Their value of the C−S−S−C dihedral angle, θ, relies on the number of methylene groups within the ring. Comparison of experimental absorbance maxima and the value of θ in energy-minimized structures produces a sinusoidal curve (Figure 1A). An analogous plot of computational absorbance maxima leads to a nearly superimposable curve (Figure 1B). The agreement between the experimental and computational absorbance maxima is evident (Figure 1C). Moreover, both the experimental and the computational data fit well to a sinusoidal function

$$\lambda_{max}(\theta) = A - B \sin|\theta| + C \sin 2|\theta| \quad (1)$$

where $-90° \leq \theta \leq 90°$.[31] Equation 1 enables the prediction of θ based on the value of λ_{max}.[32] This capability is analogous to that enabled by the Karplus equation, which is an empirical sinusoidal function that describes the relationship between H−C−C−H dihedral angles and $^3J_{H,H}$ coupling constants observed with NMR spectroscopy.[33,34]

Natural transition orbitals provide an intuitive depiction of the re-organization of electron density between a ground state and an excited state. We visualized the $S_0 \rightarrow S_1$ transition of cyclic disulfides containing 1−6 methylene groups. As shown in Figure 2, the highest occupied molecular orbital is

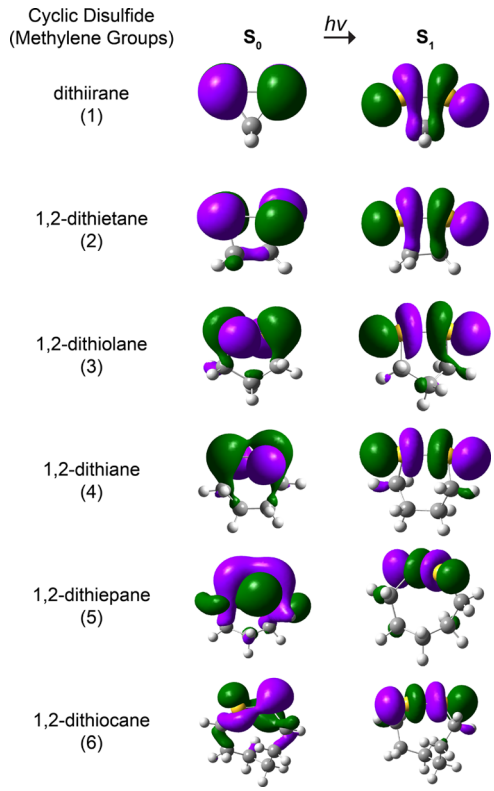

Figure 2. Images of the natural transition orbitals for the excitation of cyclic disulfides containing 1−6 methylene groups, as calculated at the M06-2X/6-311+G(d,p) level of theory.

composed of the lone pair located on sulfur with additional contributions from atoms α and (to a lesser extent) β to the sulfur atoms. Increasingly eclipsed conformations of disulfide bonds have markedly lower electron density on methylene group α to sulfur, indicating that their S_0 states are destabilized by less efficient overlap. These orbital depictions are consistent with the experimental and computational correlation depicted in Figure 1. As $\theta \rightarrow 0$, hyperconjugative interactions with groups

https://dx.doi.org/10.1021/acs.jpcb.0c02272
J. Phys. Chem. B 2020, 124, 3931−3935

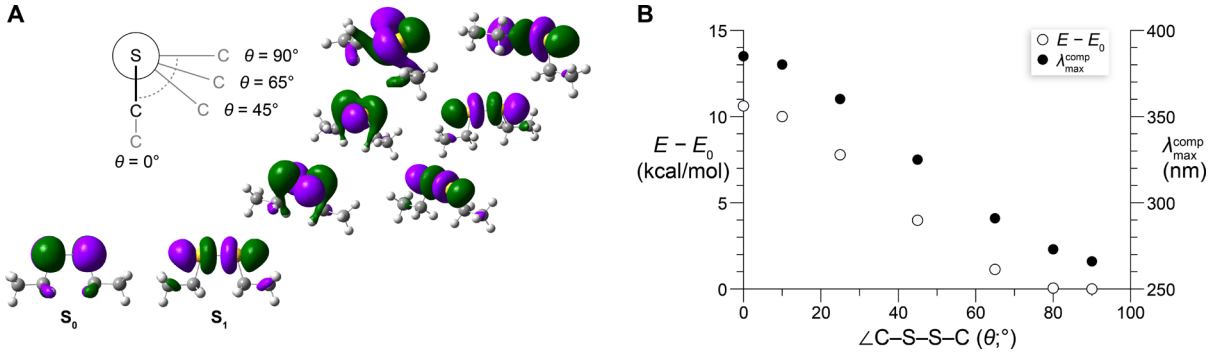

Figure 3. Effect of the C−S−S−C dihedral angle on the energetics of diethyl disulfide. (A) Images of the natural transition orbitals of $\mathbf{S_o}$ and $\mathbf{S_1}$ states. (B) Graph of computed conformational constraint energies and absorbance maxima versus C−S−S−C dihedral angles. Calculations were at the M06-2X/6-311+G(d,p) level of theory.

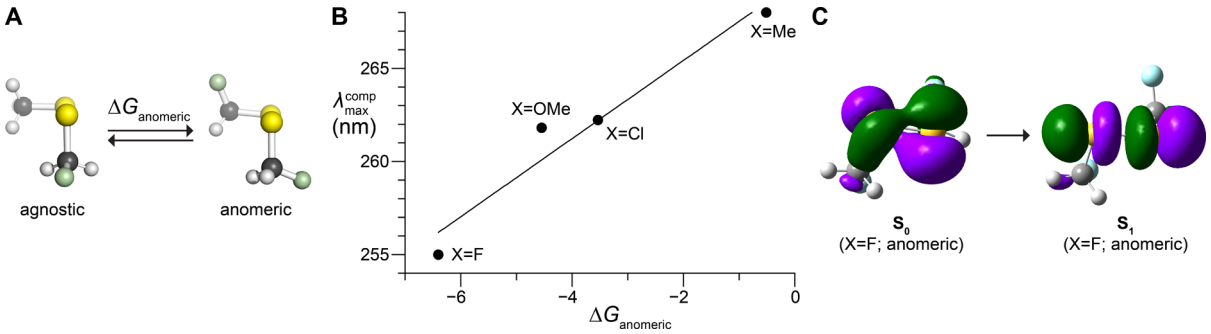

Figure 4. Anomeric effects on the energetics of disulfide bonds. (A) Conformations of XCH_2−S−S−CH_2X that disfavor or favor an anomeric effect (here, $n_S \rightarrow \sigma^*_{C-F}$). (B) Graph of computed absorbance maxima versus computed changes in free energy upon adoption of an anomeric conformation. (C) Images of the natural transition orbitals for the excitation of FCH_2−S−S−CH_2F. Calculations were at the M06-2X/6-311+G(d,p) level of theory.

α to sulfur are diminished, and electron−electron repulsion from the sulfur lone-pair electron density is enhanced. Hence, the energy of the HOMO is increased, and the energy of the photon required for the $\mathbf{S_0} \rightarrow \mathbf{S_1}$ transition is decreased. We conclude that the excitation is tunable via the dihedral angle of the disulfide bond and that hyperconjugative interactions could provide a means to tune the properties of disulfide bonds.

Next, we examined a larger range of θ values using an acyclic disulfide. Specifically, we optimized diethyl disulfide with constraints on its C−S−S−C dihedral angle (Figure 3A). TD−DFT calculations revealed that the excitation energy is dependent on the value of θ. Inspection of the natural transition orbitals for $\mathbf{S_0} \rightarrow \mathbf{S_1}$ transitions revealed that sulfur lone pairs interact less efficiently with α methylene groups in more eclipsed conformations (Figure 3A). The $\mathbf{S_0}$ orbitals of diethyl disulfide at $\theta = 0$ and 45° are similar to those of the cyclic dithiirane and 1,2-dithietane, although the sulfur lone pairs appear to mix more efficiently with surrounding moieties in the cyclic systems, perhaps because of differences in C−S−S bond angles.

Then, we searched for a correlation of $E - E_0$, which is the conformational constraint energy, and the value of θ. We found that the value of $E - E_0$ is mirrored by the energy of a photon required to elicit the $\mathbf{S_0} \rightarrow \mathbf{S_1}$ transition (Figure 3B). This correlation describes the origin of the experimental data (Figure 1A) and suggests that perturbation of the local electronic environment influences the properties of the disulfide chromophore. The low energy conformation has a value of θ near ±90°, which is the C_i^{β}−S_i^{γ}−S_k^{γ}−C_k^{β} dihedral angle (χ^3) commonly observed for disulfide bonds in proteins,[35,36] even those formed by vicinal cysteine residues.[37] When $\chi^3 = \theta = \pm 90°$, eq 1 and the parameters from Figure 1 predict values of $\lambda_{max} = A - B = 257$ nm (experimental data) or 262 nm (computational data). These values are in gratifying agreement with the known absorbance of cystine residues in proteins at ∼260 nm.[38]

We reasoned that compounds with more eclipsed C−S−S−C dihedral angles would have smaller molar absorptivity because of less overlap between the orbitals in their $\mathbf{S_0}$ and $\mathbf{S_1}$ states (Figure 2). We found that both the experimental extinction coefficient at λ_{max} and the computed oscillator strength do indeed decrease with increasing C−S−S−C dihedral angle (Figure S2A,B). Furthermore, we measured the absorptivity of oxidized lipoic acid and oxidized dithiothreitol in solutions of different dielectric constants. We observed an inverse relationship—absorptivity decreases by twofold in polar solvents (Figure S2C), presumably because of subtle perturbations to transition dipole moments. The higher absorptivity of disulfide bonds in nonpolar environments could facilitate the analysis of disulfide bonds in the hydrophobic core of folded proteins. In comparison to absorptivity, the wavelength of maximal absorbance of disulfide bonds is insensitive to the solvent polarity or protic/aprotic character.[39]

Finally, we sought a means to determine if hyperconjugative interactions between the sulfur lone pairs and α substituents could influence the $\mathbf{S_0} \rightarrow \mathbf{S_1}$ excitation energy. The anomeric effect is a well-known example of a hyperconjugative interaction that stabilizes molecular conformations and influences chemical reactivity.[40−42] We asked whether the

https://dx.doi.org/10.1021/acs.jpcb.0c02272
J. Phys. Chem. B 2020, 124, 3931−3935

conformation of an X-substituted dimethyl disulfide could benefit from an anomeric effect, in which the sulfur lone pair donates electron density into the σ^* orbital of the C−X bond (Figure 3A). Specifically, we considered substituted dimethyl disulfides with the formula $XH_2C-S-S-CH_2X$ and X = Me, F, Cl, or OMe. We computed optimized structures in a conformation that would benefit from the anomeric effect and in an agnostic one (Figure 4A). We performed TD−DFT calculations to assess the excitation maxima of the disulfides in their anomeric conformation. We found that the difference in free energy between the anomeric and agnostic conformations ($\Delta G_{anomeric}$) correlates with the excitation wavelength maximum in the anomeric conformation (Figure 4B). This correlation supports the stabilization of $\mathbf{S_0}$ as being an effective mechanism for increasing the energy needed to elicit the $\mathbf{S_0}\rightarrow\mathbf{S_1}$ transition. Inspection of the natural transition orbitals for the $\mathbf{S_0}$ ground state reveals that substitution at the anomeric position redistributes electron density into the σ^*_{C-X} orbital (Figure 4C). Together, these results indicate that stereoelectronic effects can perturb the photophysical properties of disulfide bonds.

■ CONCLUSIONS

We conclude that the photophysical properties of disulfide bonds are predictable and manipulatable. The absorbance maximum arises from electron−electron repulsion, which increases the energy of the $\mathbf{S_0}$ state at C−S−S−C dihedral angles approaching $\theta = 0°$. Secondary orbital interactions can modify the absorbance maximum further. In particular, an anomeric effect can be induced by stabilization of the $\mathbf{S_0}$ state. Finally, the C−S−S−C dihedral angle of a disulfide can be estimated simply from its absorbance maximum.[32]

■ ASSOCIATED CONTENT

Supporting Information

The Supporting Information is available free of charge at https://pubs.acs.org/doi/10.1021/acs.jpcb.0c02272.

Physical and photophysical properties of disulfides, atomic coordinates of disulfides, anomeric conformations of $XH_2C-S-S-CH_2X$, agnostic conformations of $XH_2C-S-S-CH_2X$, and UV−vis spectra (PDF)

■ AUTHOR INFORMATION

Corresponding Author

Ronald T. Raines − *Department of Chemistry, Massachusetts Institute of Technology, Cambridge, Massachusetts 02139, United States;* orcid.org/0000-0001-7164-1719; Email: rtraines@mit.edu

Author

Henry R. Kilgore − *Department of Chemistry, Massachusetts Institute of Technology, Cambridge, Massachusetts 02139, United States*

Complete contact information is available at: https://pubs.acs.org/10.1021/acs.jpcb.0c02272

Notes

The authors declare no competing financial interest.

■ ACKNOWLEDGMENTS

This paper is dedicated to Martin Karplus on the occasion of his 90th birthday. We are grateful to Prof. M. Movassaghi and C. R. Olsson for inspirational discussions, and we thank Dr. Brian J. Levandowski for helpful comments on the manuscript. This work was supported by Grant R01 GM044783 (NIH) and made use of the Extreme Science and Engineering Discovery Environment (XSEDE), which is supported by grant number ACI-1548562 (NSF).

■ REFERENCES

(1) Buchner, J.; Moroder, L. *Oxidative Folding of Peptides and Proteins*; Royal Society of Chemistry: Cambridge, U.K., 2009.

(2) Fass, D. Disulfide Bonding in Protein Biophysics. *Annu. Rev. Biophys.* **2012**, *41*, 63−79.

(3) Poole, L. B. The Basics of Thiols and Cysteines in Redox Biology and Chemistry. *Free Radic. Biol. Med.* **2015**, *80*, 148−157.

(4) Yang, J.; Carroll, K. S.; Liebler, D. C. The Expanding Landscape of the Thiol Redox Proteome. *Mol. Cell. Proteomics* **2016**, *15*, 1−11.

(5) Bechtel, T. J.; Weerapana, E. From Structure to Redox: The Diverse Functional Roles of Disulfides and Implications in Disease. *Proteomics* **2017**, *17*, 1600391.

(6) Fass, D.; Thorpe, C. Chemistry and Enzymology of Disulfide Cross-Linking in Proteins. *Chem. Rev.* **2018**, *118*, 1169−1198.

(7) Góngora-Benítez, M.; Tulla-Puche, J.; Albericio, F. Multifaceted Roles of Disulfide Bonds: Peptides as Therapeutics. *Chem. Rev.* **2014**, *114*, 901−926.

(8) Zhao, B.-C.; Lin, H. C.; Yang, D.; Ye, X.; Li, Z.-G. Disulfide Bridges in Defensins. *Curr. Top. Med. Chem.* **2016**, *16*, 206−219.

(9) Huang, Y.-H.; Du, Q.; Craik, D. J. Cyclotides: Disulfide-Rich Peptide Toxins in Plants. *Toxicon* **2019**, *172*, 33−44.

(10) Kim, J.; Movassaghi, M. Biogenetically-Inspired Total Synthesis of Epidithiodiketopiperazines and Related Alkaloids. *Acc. Chem. Res.* **2015**, *48*, 1159−1171.

(11) Dunbar, K. L.; Scharf, D. H.; Litomska, A.; Hertweck, C. Enzymatic Carbon−Sulfur Bond Formation in Natural Product Biosynthesis. *Chem. Rev.* **2017**, *117*, 5521−5577.

(12) Wang, N.; Saidhareddy, P.; Jiang, X. Construction of Sulfur-Containing Moieties in the Total Synthesis of Natural Products. *Nat. Prod. Rep.* **2020**, *37*, 246−275.

(13) Bergson, G.; Claeson, G.; Schotte, L.; Block-Bolten, A.; Toguri, J. M.; Flood, H. Ultraviolet Absorption Spectra of Saturated Disulphides and Diselenides. *Acta Chem. Scand.* **1962**, *16*, 1159−1174.

(14) Van Wart, H. E.; Lewis, A.; Scheraga, H. A.; Saeva, F. D. Disulfide bond dihedral angles from Raman spectroscopy. *Proc. Natl. Acad. Sci. U.S.A.* **1973**, *70*, 2619−2623.

(15) Chivers, P. T.; Prehoda, K. E.; Raines, R. T. The CXXC Motif: A Rheostat in the Active Site. *Biochemistry* **1997**, *36*, 4061−4066.

(16) Weik, M.; Ravelli, R. B. G.; Kryger, G.; McSweeney, S.; Raves, M. L.; Harel, M.; Gros, P.; Silman, I.; Kroon, J.; Sussman, J. L. Specific Chemical and Structural Damage to Proteins Produced by Synchrotron Radiation. *Proc. Natl. Acad. Sci. U.S.A.* **2000**, *97*, 623−628.

(17) Schmidt, B.; Ho, L.; Hogg, P. J. Allosteric Disulfide Bonds. *Biochemistry* **2006**, *45*, 7429−7433.

(18) Kilgore, H. R.; Raines, R. T. $n\rightarrow\pi^*$ Interactions Modulate the Properties of Cysteine Residues and Disulfide Bonds in Proteins. *J. Am. Chem. Soc.* **2018**, *140*, 17606−17611.

(19) Barltrop, J. A.; Hayes, P. M.; Calvin, M. The Chemistry of 1,2-Dithiolane (Trimethylene Disulfide) as a Model for the Primary Quantum Conversion Act in Photosynthesis. *J. Am. Chem. Soc.* **1954**, *76*, 4348−4367.

(20) Whitney, R. B.; Calvin, M. Chemical and Photochemical Studies on 6,8-Thioctic Acid and 1,2-Dithiolane (Trimethylene Disulfide). *J. Chem. Phys.* **1955**, *23*, 1750−1756.

(21) Seaborg, G. T.; Benson, A. A. Melvin Calvin. In *Biographical Memoirs*; National Academy of Sciences: Washington, DC, 1998; Vol. *75*, pp 96−115.

(22) Buchanan, B. B.; Wong, J. H. A Conversation with Andrew Benson: Reflections on the Discovery of the Calvin−Benson Cycle. *Photosynth. Res.* **2013**, *114*, 207−214.
(23) Boyd, D. B. Conformational Dependence of the Electronic Energy Levels in Disulfides. *J. Am. Chem. Soc.* **1972**, *94*, 8799−8804.
(24) Ochmann, M.; Hussain, A.; von Ahnen, I.; Cordones, A. A.; Hong, K.; Lee, J. H.; Ma, R.; Adamczyk, K.; Kim, T. K.; Schoenlein, R. W.; et al. UV-Photochemistry of the Disulfide Bond: Evolution of Early Photoproducts from Picosecond X-ray Absorption Spectroscopy at the Sulfur K-edge. *J. Am. Chem. Soc.* **2018**, *140*, 6554−6561.
(25) Schnorr, K.; Bhattacherjee, A.; Oosterbaan, K. J.; Delcey, M. G.; Yang, Z.; Xue, T.; Attar, A. R.; Chatterley, A. S.; Head-Gordon, M.; Leone, S. R.; Gessner, O. Tracing the 267 nm-Induced Radical Formation in Dimethyl Disulfide using Time-Resolved X-ray Absorption Spectroscopy. *J. Phys. Chem. Lett.* **2019**, *10*, 1382−1387.
(26) Cleland, W. W. Dithiothreitol, a New Protective Reagent for SH groups. *Biochemistry* **1964**, *3*, 480−482.
(27) Critchfield, F. E.; Gibson, J. A., Jr.; Hall, J. L. Dielectric Constant for the Dioxane−Water System from 20 to 35°. *J. Am. Chem. Soc.* **1953**, *75*, 1991−1992.
(28) Frisch, M. J.; Trucks, G. W.; Schlegel, H. B.; Scuseria, G. E.; Robb, M. A.; Cheeseman, J. R.; Scalmani, G.; Barone, V.; Petersson, G. A.; Nakatsuji, H.; et al. *Gaussian 16*, Revision C.01; Gaussian, Inc.: Wallington, CT, 2016.
(29) Martin, R. L. Natural Transition Orbitals. *J. Chem. Phys.* **2003**, *118*, 4775−4777.
(30) Dennington, R.; Keith, T. A.; Millam, J. M. *GaussView*, version 6; Semichem, Inc.: Shawnee Mission, KS, 2016.
(31) Our analysis does not consider obtuse C−S−S−C dihedral angles, which are relatively rare.
(32) Using the experimental data (Figure 1A) and neglecting the third term in eq 1 (which has a relatively small coefficient) gives $\theta = \pm\arcsin[(460\ \text{nm} - \lambda_{max})/207\ \text{nm}]$.
(33) Karplus, M. Contact Electron−Spin Coupling of Nuclear Magnetic Moments. *J. Chem. Phys.* **1959**, *30*, 11−15.
(34) Karplus, M. Vicinal Proton Coupling in Nuclear Magnetic Resonance. *J. Am. Chem. Soc.* **1963**, *85*, 2870−2871.
(35) Richardson, J. S. The Anatomy and Taxonomy of Protein Structure. *Adv. Protein Chem.* **1981**, *34*, 167−339.
(36) Thornton, J. M. Disulphide Bridges in Globular Proteins. *J. Mol. Biol.* **1981**, *151*, 261−287.
(37) Richardson, J. S.; Videau, L. L.; Williams, C. J.; Richardson, D. C. Broad Analysis of Vicinal Disulfides: Occurrences, Conformations with cis or with trans Peptides, and Functional Roles Including Sugar Binding. *J. Mol. Biol.* **2017**, *429*, 1321−1335.
(38) Schmid, F.-X. Biological Macromolecules: UV−Visible Spectrophotometry. In *eLS*; Bridgewater, R., Ed.; John Wiley & Sons: Chichester, U.K., 2001; http://www.els.net.
(39) Rosenthal, N. A.; Oster, G. Ultraviolet Spectra of Alkyl Disulfides and their Relation to Alkali Cleavage of Disulfide Bonds. *J. Am. Chem. Soc.* **1961**, *83*, 4445−4448.
(40) Deslongchamps, P. *Stereoelectronic Effects in Organic Chemistry*; Pergamon Press: Oxford, U.K., 1983.
(41) Kirby, A. J. *Stereoelectronic Effects*; Oxford University Press: Oxford, U.K., 1996.
(42) Alabugin, I. V. *Stereoelectronic Effects: A Bridge Between Structure and Reactivity*; John Wiley & Sons: Chichester, U.K., 2016.

https://dx.doi.org/10.1021/acs.jpcb.0c02272
J. Phys. Chem. B 2020, 124, 3931−3935